# Model of Total Suspended Solid (TSS) distribution due to coastal mining in Western Coast of Kundur Island part of Berhala Strait

# Model of Total Suspended Solid (TSS) distribution due to coastal mining in Western Coast of Kundur Island part of Berhala Strait

**I W Nurjaya[1*], H Surbakati[2] and N M N Natih[1]**

[1]Department of Marine Science and Technology, Faculty of Fisheries and Marine Science, Bogor Agricultural University, Bogor, Indonesia
[2]Marine Science Program, University of Sriwijaya, Indonesia

*E-mail: i.wayan.nurjaya@apps.ipb.ac.id

**Abstract.** The Berhala Strait is located between the islands of Sumatra and Kundur Island with natural resources on the seabed in the form of lead. One of the state-owned mining companies is PT Tambang Timah that has the authorization to exploit lead on the west coast of Kundur Island. Typical oceanographic conditions of Total Suspended Solid (TSS) range from 35-37 mg/L, naturally large rivers that flow into the east coast of Sumatra contributed to the increase of TSS. Indications of the process can be seen from the range of surface salinity in these waters ranging from 25.5-28.0 psu. Mining activities at coastal waters have the high potential to increase turbidity in the water column. The scenario in this TSS distribution model is based on 2D-hydrodynamics model. The increase of TSS within the seawater is caused by the operation of dredgers (6 units) and suction vessels (11 units). TSS Model is built for two different monsoons, the northeast and southeast monsoons. Lead/metal mining activities in the west coast waters of Kundur Island cause an increasing TSS concentration up to 90-100 mg/L. TSS distribution patterns from mining activities will be explained simultaneously in 2 different monsoons.

**Keywords**: Berhala Strait, monsoon, suction vessels, total suspended solid, turbidity

## 1. Introduction

An understanding of the processes and functions of the sea is needed in order to utilize and explore marine resources, both biological resources and not, such as sea sand mining and mineral exploration in the sea floor. Oceanographic information and data are needed both in relation to the operational optimization and work safety at sea and in predicting the damage that will be caused through a pattern of turbidity distribution.

Some potential damages or disturbances arising from sand or mineral mining activities are an increase in water turbidity. It can block the amount of light penetration into deeper layers so that photosynthesis is not optimal. Damage to the basic habitat that is generally inhabited by benthic organisms is also threatened, so that the condition of the food chain in these waters becomes disrupted [1-4]. Another possibility is the resuspension of toxic substances from sediment deposits on the seabed due to stirring by cutting, stirring and suction processes [5, 6].

Naturally, sources of turbidity originate from a freshwater discharge into the sea. Indonesia has large rivers flowing into the sea, almost all streams of these rivers carry sediment into the coastal waters,

causing increased turbidity, sedimentation and silting of water bodies. In the western coast of Kundur Island high turbidity originates from the eastern mainland of Sumatra Island. Variations in the size of dissolved sediment granules vary greatly so that the deposition location will depend on the size of particle. Generally, finer-sized granular particles will stay longer in the water column so that they are further distributed from the source, whereas larger ones tend to settle closer.

Economic activities in sea often increase human activities in sea such as dredging, reclamation, installation of pipes and cables under the sea and sea sand mining. These activities have the potential to cause an increase in turbidity. One of the activities that will be described in this paper is lead mining in the west coast waters of Kundur Island.

## 2. Data Analysis

### *2.1. Study location*

Geographically the study location is located on the west coast of Kundur Island, Indonesia which borders the Berhala Strait and the Malacca Strait (figure 1). The geographical position has the potential to receive low-salinity water input that flows from the estuaries found on the east coast of Sumatra, especially in Riau.

### *2.2. Materials and Methods*

Data on Temperature, Salinity, Conductivity, Sound velocity, Beam transmission were obtained using the CTD SeaCat Profiler Type SBE 18 instrument, USA (figure 2b). Data of current speed and direction is obtained by using a current meter instrument that was installed at one point and operated for 36 hours.

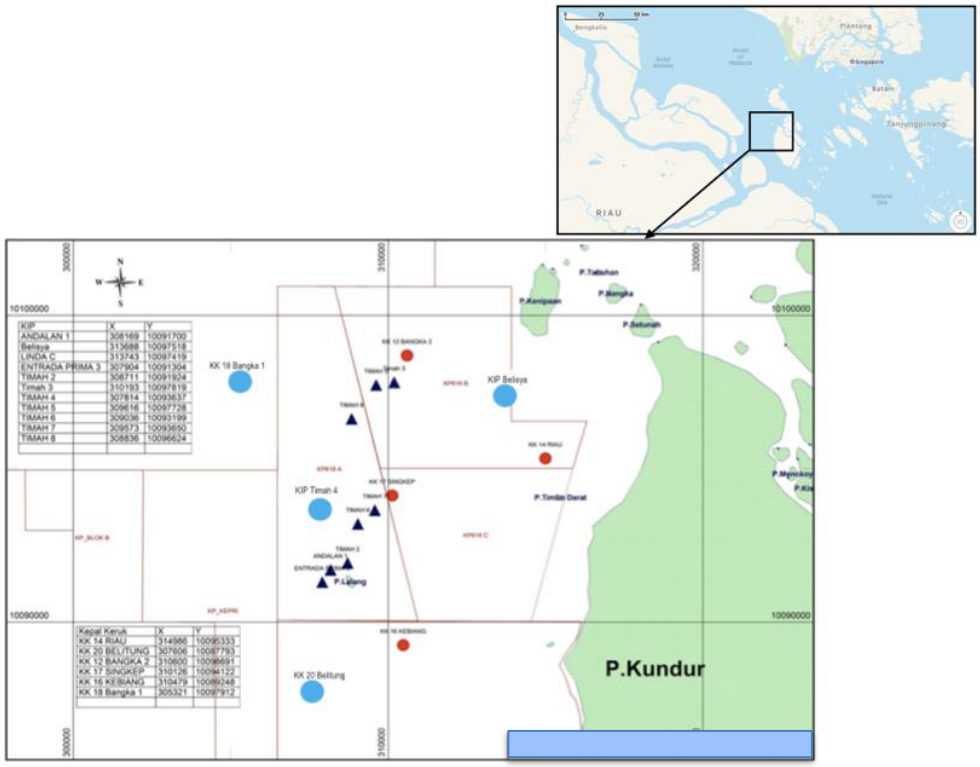


**Figure 1.** Location of study ( ), at the western coast of Kundur Island.


**Figure 2.** Transmissometer for measurement TSS (a) dan CTD Sensor for measuring conductivity and temperature according to depth (b).

Measurements were made at 96 stations in western coast of Kundur waters based on the source of impact point approach (48 stations), and the cumulative impact approach (48 stations). At the time of the survey there were 6 Dredgers (KK=Kapal Keruk) and Production Suction Ships (KIP=Kapal Isap Produksi). The KK and KIP vessels belong to PT Tambang Timah which operates on the western coast of Kundur Island tabulated on table 1 and described on figure 1. The KK and KIP operate close to each other and some are operating separately relatively far from the others.

**Table 1.** Dredger (KK) and Production Suction Vessels (KIP) Operating in the West Waters of Kundur Island on July 22 - 29, 2012.

| No | Lon | Lat | Vessel Type | Name/Identity |
|---|---|---|---|---|
| 1 | 310600 | 98691 | Dredger | KK-12, Bangka 2 |
| 2 | 314986 | 95333 | Dredger | KK-14, Riau |
| 3 | 310479 | 89248 | Dredger | KK-16, Kebiang |
| 4 | 310126 | 94122 | Dredger | KK-17, Singkep |
| 5 | 305321 | 97912 | Dredger | KK-18, Bangka 1[1)] |
| 6 | 307606 | 87793 | Dredger | KK-20, Belitung[1)] |
| 7 | 308169 | 91700 | Production Suction Vessels | KIP-ANDALAN |
| 8 | 313688 | 97518 | Production Suction Vessels | Belisya[1)] |
| 9 | 313743 | 97419 | Production Suction Vessels | LINDA-C |
| 10 | 307904 | 91304 | Production Suction Vessels | Entrada |
| 11 | 308711 | 91924 | Production Suction Vessels | Timah-2 |
| 12 | 310193 | 97819 | Production Suction Vessels | Timah-3 |
| 13 | 307814 | 93637 | Production Suction Vessels | Timah-4[1)] |
| 14 | 309616 | 97728 | Production Suction Vessels | Timah-5 |
| 15 | 309036 | 93199 | Production Suction Vessels | Timah-6 |
| 16 | 309573 | 93650 | Production Suction Vessels | Timah-7 |
| 17 | 308836 | 96624 | Production Suction Vessels | Timah-8 |

[1)] *KK / KIP operations selected for measurement with a single point source of impact approach*

The single point source of impact approach is used to measure the individual impact of the KK/KIP operating. The cumulative impact approach is used to measure the cumulative impact of all dredges/production vessels (KK/KIP) operating in the western coast of Kundur Island.

a) *Single point source of impact*

To find out the single point source of impact characters of individual KK/KIP, the measurement focused on four ships operating far apart from the others. The intended vessel is Belitung KK, Bangka- KK, KIP Timah-4, and Belisya KIP (figure 1). These four vessels are referred to as KK/KIP samples. In each KK/KIP sample, measurement stations are determined under the following systems:

- Two measurement stations were carried out in upward of the current, located 50m and 500m from the KK/KIP position
- Six measurement stations were carried out at the downward of the current direction, 100, 200, 300, 500, 1000 and 1500 m from the KK/KIP position.
- Two stations were measured to the right of KK/KIP (100 and 300 m).
- Other two stations were measured at 100m and 300 m to the left of KK/KIP location.

b) *Cummulative impact approach*

To measure the cumulative impact from 17 KK/KIP operating in the western coast waters of Kundur Island, 48 stations were measured under the following systems:

- All operational areas of PT Tambang Timah in the western waters of Kundur which are in DU 618 and DU 621, plus the surrounding coastal areas, are assumed to be affected by the cumulative impact of the operations of the 7 KK/KIP PT Tambang Timah. This cumulative impact area stretches over an area of 12 km x 48 km. In this area the cumulative impact is made by a 4 km x 4 km virtual transect.
- At each end of the 4 km x 4 km water room 48 stations/locations for measuring data were determined. In total there were 48 stations measuring the cumulative impacts in an area of 12 km x 48 km.

*2.3. Calculation of TSS concentration from production suction vessels*

Excavation capacity: 150 $m^3$/hour: sand 52.45%, dust 25.34%, clay 22.31%. The percentage, the fine sediment fraction = 47.65% x 150 $m^3$/hour = 71,475 $m^3$. Weight: 2,650 kg/$m^3$ x 71,475 $m^3$: 189,408.8 kg = 9,40 tons. Assuming that 20% of the fine sediment fraction would be suspended, then = 0.2 x 189,408.8 kg = 37,881.75 kg. The TSS volume would experience mixing with seawater. The volume of seawater that functions as a diluent are calculated by considering the tidal period, current velocity and wave amplitude. Tidal period = 6 hours current speed = 0.3 m/sec. So the distribution distance is: = 0.3m/sec x 6 hours x 3,600 sec/hour = 6,480 m/6 hours. Wihtin one hour, distance (1 hour) = 6,480 m/6 hours = 1,080 m.

The sediment would spread in the sea according to the tidal excursion in the form of an ellipse. So that the area of TSS distribution is calculated by the formula: area = $\prod r^2$ = 3.14 x (1,080 m)$^2$ = 3.662.496 $m^2$; volume = area ($m^2$) x depth (5 m) = 3,66 ,496 $m^2$ x 5 m = 18, 312,480 $m^3$; TSS concentration = TSS/volume of water = 37, 881.75 / 18,312,480 = 0.002069 kg/m or 2.0690 mg/L.

To find out the distribution of turbidity values due to the disposal of KK and KIP tailing is used as follows:

*2.4. Hydrodynamic model*

The equations used in this model are continuity equations and momentum equations with depth averages. This model uses the finite difference method approach to solve the equations used.

*2.4.1. Model of suspended sediment distribution.* The suspended sediment distribution model was built using the 2007 version of the MIKE 21 MT module developed by DHI water and environment, Denmark. Sediment transport was accomplished using the advection-dispersion equation. The equation can be written as follows:

$$\frac{\partial \bar{c}}{\partial t} + u\frac{\partial \bar{c}}{\partial x} + v\frac{\partial \bar{c}}{\partial y} = \frac{1}{h}\frac{\partial}{\partial x}\left(hD_x\frac{\partial \bar{c}}{\partial x}\right) + \frac{1}{h}\frac{\partial}{\partial y}\left(hD_y\frac{\partial \bar{c}}{\partial y}\right) + Q_L C_L \frac{1}{h} - S \quad (1)$$

Notes:

| | | |
|---|---|---|
| $\bar{c}$ | : | averaged concentration of depth (kg/m$^3$) |
| $u, v$ | : | average flow velocity to depth (m/s) |
| $D_x, D_y$ | : | dispersion coefficient (m$^2$/s) |
| $h$ | : | water depth (m) |
| $S$ | : | acresion/erosion (kg/m$^3$/s) |
| $Q_L$ | : | source debit per unit area horizontally (m$^3$/s/m$^2$) |
| $C_L$ | : | source concentration (kg/m$^3$) |

The advection-dispersion equation is resolved explicitly with a third-order finite difference approach, known as the ULTIMATE scheme (1) [13].

The deposition rate is expressed by the equation (2) [14]:

$$S_D = w_s c_b p_d \quad (2)$$

Notes:

| | | |
|---|---|---|
| $S_D$ | : | deposition rate |
| $w_s$ | : | Sediment fall Velocity (m/s) |
| $c_b$ | : | subsurface concentration (kg/m$^3$) |
| $p_d$ | : | deposition probability $= 1 - \frac{\tau_b}{\tau_{cd}}$ , $\tau_b \leq \tau_{cd}$ |
| $\tau_b$ | : | bed shear stress (N/m$^2$) |
| $\tau_{cd}$ | : | critical bed shear stress for deposition (N/m$^2$) |

Mehta *et al.* (1989), describes the basic erosion rate with the following equation (3):

$$S_E = E\left(\frac{\tau_b}{\tau_{ce}} - 1\right), \quad \tau_b > \tau_{ce} \quad (3)$$

Notes:

| | | |
|---|---|---|
| $E$ | : | seabed erodibility (kg/m$^2$/s) |
| $\tau_{ce}$ | : | critical bed shear stress for erosion (N/m$^2$) |

*2.5. Sediment settling velocity*

Sediment settling velocity is formulated by equation below (4) [15-17]:

$$w = \begin{cases} \dfrac{(s-1)gd^2}{18v} & d < 100\mu m \\ \dfrac{10v}{d}\left\{\left[1 + \dfrac{0.01(s-1)gd^3}{v^2}\right]^{0.5} - 1\right\} & 100 < d \leq 1000\mu m \\ 1.1[(s-1)gd]^{0.5} & d > 1000\mu m \end{cases} \quad (4)$$

*2.6. Data input*

*2.6.1. Tide data.* Tidal data was used as an open boundary condition using forecasting data obtained from High Resolution Global Tidal Prediction with 15 minutes resolution. The tidal data obtained was then interpolated to be every 10 seconds (according to the step time/time simulation step) using cubic spline to obtain stability in the model.

*2.6.2. Wind data.* Wind data was used using ECMWF prediction data with a spatial resolution of 1.5 ° x 1.5 ° and data intervals every 3 hours. Wind data used as input to the model was January data (West season) and July data (East season). The dominant wind in the west season is the wind that blows from the North and Northeast, while in the east season, the dominant wind blows from the Southeast (figure 3).

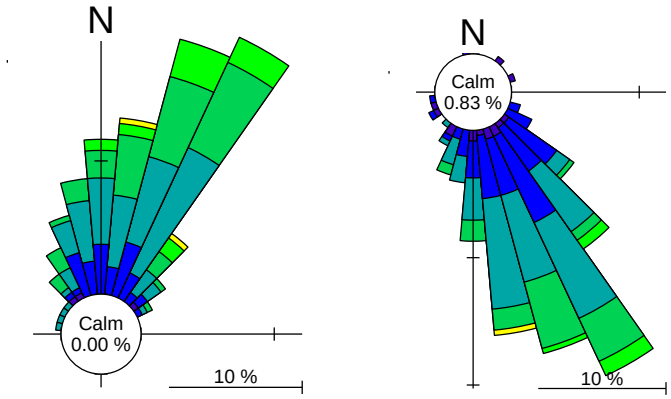


(a) (b)

**Figure 3.** Wind Rose North East Monsoon (a) and South East Monsoon (b), wind speed (m/s): = above 7, = 6-7, = 5-6, = 4-5, = 3-4, = 2-3, = 1-2, = below 1.

*2.6.3. Bathymetry data.* Bathymetry data used as input data in the model area (domain area model) was bathymetry data map No: 13 scale of 1: 200,000; No: 105 scale of 1: 100,000 and No: 13 A map with a scale of 1: 25,000 from Hydro-Oceanographic Service of the Indonesian Navy (PUSHIDROSAL = Pusat Hidrografi dan Oseanografi Angkatan Laut). Figure 4 shows the bathymetry map in the model area (domain model) plotted in depth data from map digitization results No. 81A and 84. Modeling was done with Nested area modeling, namely modeling for large and small scales modeling (the box around Kundur Island).

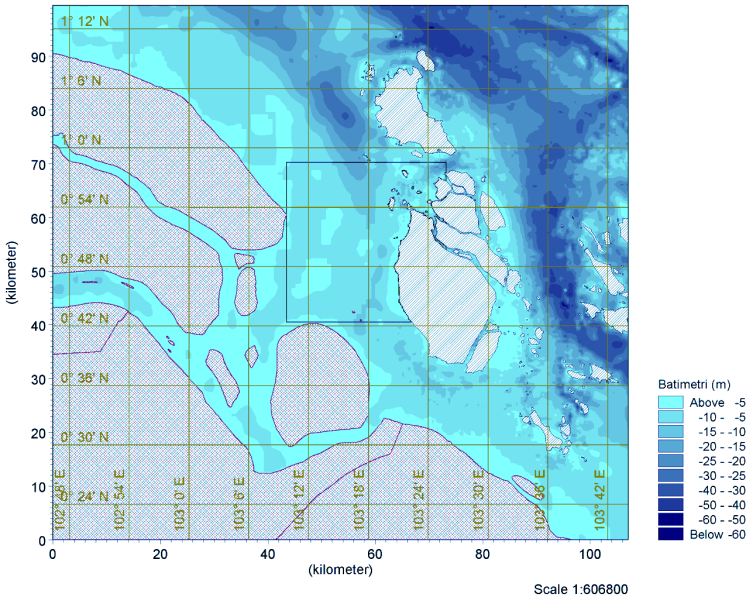


**Figure 4.** Bathymetry map of the study area and its around.

To find out the distribution of turbidity values both inside WIUP and outside WIUP will use the Surfer method. With this method, we will describe the distribution of various values of turbidity in two dimensions.

## 3. Results and Discussion

The waters in the west coast of Kundur Island are shallow coastal waters located directly adjacent to the mouth of the Malacca Strait in the north, the strait between the Karimun Besar Island and Kundur Island which borders the Singapore Strait in the northeast. In the south bordering the Berhala Strait and the waters of the Lingga Islands. This border area generally has unique physical characteristics both as an area between tidal propagation from the Indian Ocean through the Malacca Strait and tidal propagation from the Pacific Ocean through the South China Sea and Singapore Strait. In order to understand the oceanographic physics characteristics of Kundur coastal waters, especially around the location of the activity, the following parameters will be described.

Variations in the depth of the coastal waters are illustrated by different color scales, as presented on the right side of the image (figure). The shallower waters are characterized by light blue, the deeper is depicted in dark blue. The water depth at the location of PT Tambang Timah ranges between 5-24 m. The deeper water depths are found in the northern part of the location to the west coast of the Karimun Besar Island, the depth can reach 50 m. Based on wind conditions that are predominantly influenced by the season, generally the wave height in each season also varies (table 2).

**Table 2.** Seasonal wave conditions in the western coast waters of Kundur Island.

| Period | Wind direction | Velocity (knot) | Wave height (m) |
|---|---|---|---|
| Dec-Jan-Feb | N-NE-E | 4-8 | 0.3 – 0.5 |
| Mar-Apr- May | NE-E-SE | 4-7 | 0.3 – 1.0 |
| Jun-Jul-Aug | SE-S-SW-W | 5-9 | 0.3 – 0.6 |
| Sep-Oct-Nov | SW-W-NW | 3-7 | 0.5 – 1.0 |

During the northeast season (north-east monsoon) in December-February or the west season in the Java Sea, the wind speed was 4-8 knots dominantly blowing from the north, northeast and east. It is able to produce surface waves ranging from 0.3 - 0.5 m.

The wind pattern totally reverses when entering the southeast season (south-east monsoon) June-August or east season in the Java Sea. During this southeast season the dominant winds blow from the southeast, southwest and from the south with wind speeds of 5-9 knots. Surface waves that can be raised in the southeast season range from 0.3 - 0.6 m.

The western coast waters of Kundur Island which is located adjacent to the mouth of the southern Malacca Strait and the mouth of the Strait of eastern Singapore and the waters of the northwestern part of the Karimata Strait and Riau Strait have a complex influence in the spread of tidal waves originating from the Indian Ocean, Pacific Ocean. In figure 5, there is a fluctuation in sea level for the month of February 2010. The highest tidal range in the month could reach 3.1 m.

On figure 6 it is clear to see that tidal propagation originates from the Indian Ocean through the Andaman Sea and Malacca Strait. This was indicated by the presence of sea level that rose first at Tanjung Balai then followed by rising sea levels in Tanjung Balai and Singapore.

Currents in the waters are generated by various generating forces such as wind, tides, differences in water density, and hydrostatic pressure of the water. The magnitude of the influence of each of the current generation forces on the strength and direction of the current flow caused is dependant on the type of waters (beaches, bays and the high seas) and their geographical conditions.

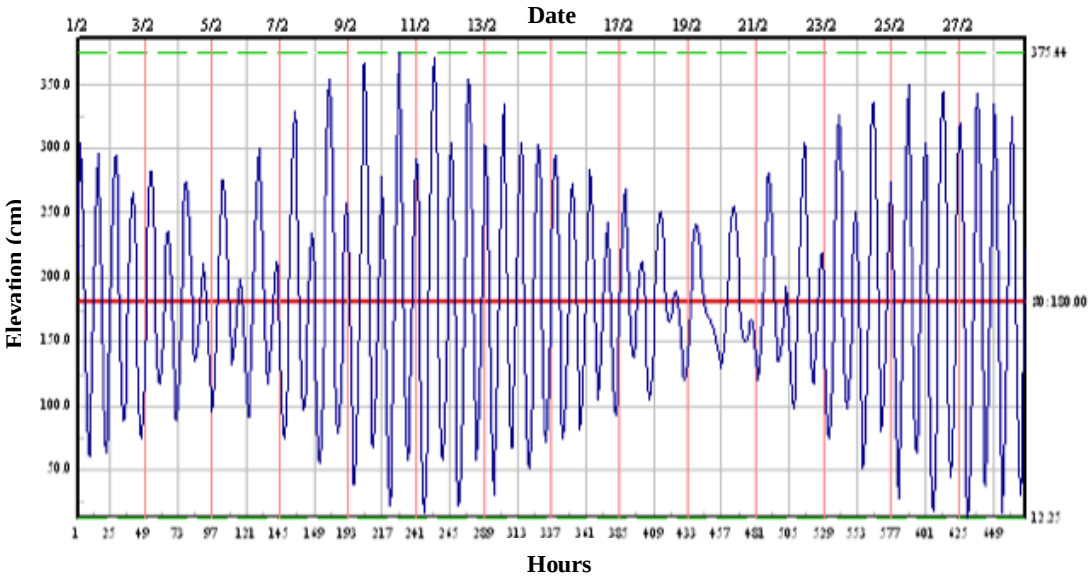


**Figure 5.** Sea level fluctuation on February 2010 plotted from tidal data prediction derived from measurement at the StationTanjung Balai Karimun (Pushidrosal).

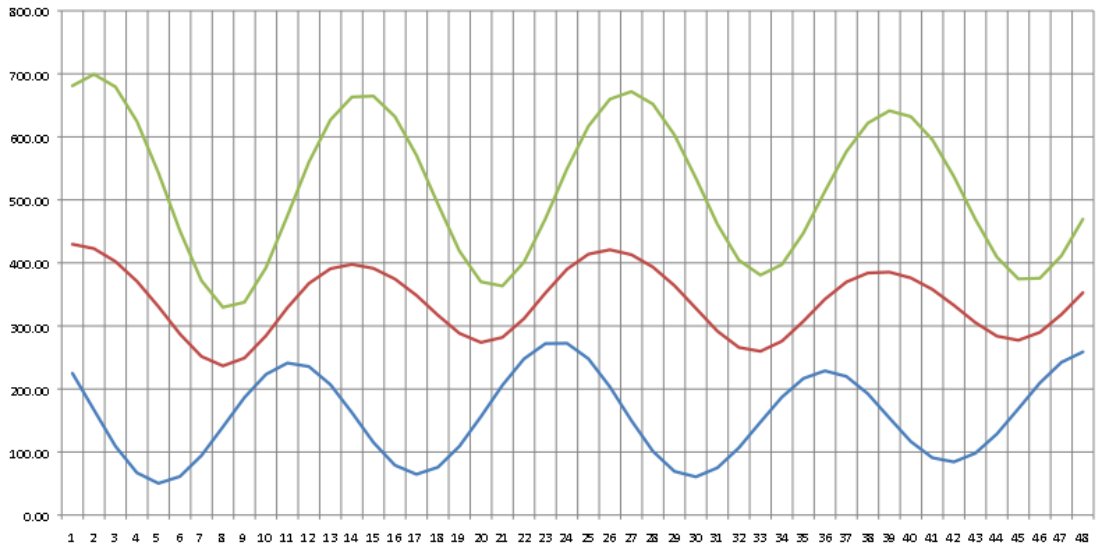

**Figure 6.** Comparing tidal fluctuation from 3 different tidal stations: blue = Kuala Tanjung Asahan, red = Tanjung Balai Karimun, green = Singapura.

Monsoonal system of the South East Asian waters can be grouped into 4, namely the northeast monsoon that occurs in December-February, first transition in March-May, southeast Monsoon occurred in June-August, and the second transition in September-November. Significantly, these four different groups can distinguish wind patterns that occur over Indonesian waters. When the northeast monsoon takes place, the dominant wind blows from the northeast and is then deflected east over the waters of the Java Sea. In contrast to the southeastern monsoon, the wind turned totally blowing from the southeast or from the top of the Australian continent then deflected west over the waters of the Java Sea and finally turned northeast over the waters of Riau Islands.

The difference in surface-based wind patterns results in differences in surface flow patterns such as examples of wind-driven circulation patterns. Surface currents in the northeast monsoon tend to be in line with the wind pattern that is moving from the waters of the South China Sea to the Java Sea. In the southeast monsoon the surface current pattern moves in opposite directions, namely from the waters of the Java Sea out into the waters of the South China Sea [7].

In situ current measurements were conducted for model validation. Current simulations were derived from hydrodynamic model. Input data used to run model was bathymetry, wind and tides. These three factors have the most roles in determining the currents in the sea. Considering that Indonesian waters including Kundur are very strongly influenced by the monsoon, this was considered in this simulation scenario, namely the west and east seasons. Data input parameters that also change based on time are tides, therefore another scenario made in this current model was that there were 4 scenarios, namely the current pattern when the sea level is in the MSL (Mean Sea Level) towards the highest tide point, when sea level is at the highest tide, when sea level at MSL goes to the lowest ebb and when the sea level is at the lowest ebb.

Surface temperatures measured by CTD ranged from 29.0- 29.8$^{o}$C. The higher water temperatures were measured around Tanjung Balai Karimun (29.7$^{o}$C), at the south - the west coast of Kundur Island the water temperature decreased to 29.4$^{o}$C. Lowest surface temperatures were measured in the north-northwest part of Kundur, it is 29.2$^{o}$C (figure 7a). Cross section of seawater temperature from the south to the north is shown in figure 7b. The warmer temperatures (red color) occupied the upper layer on the north side, while the cooler ones in the deeper layer.

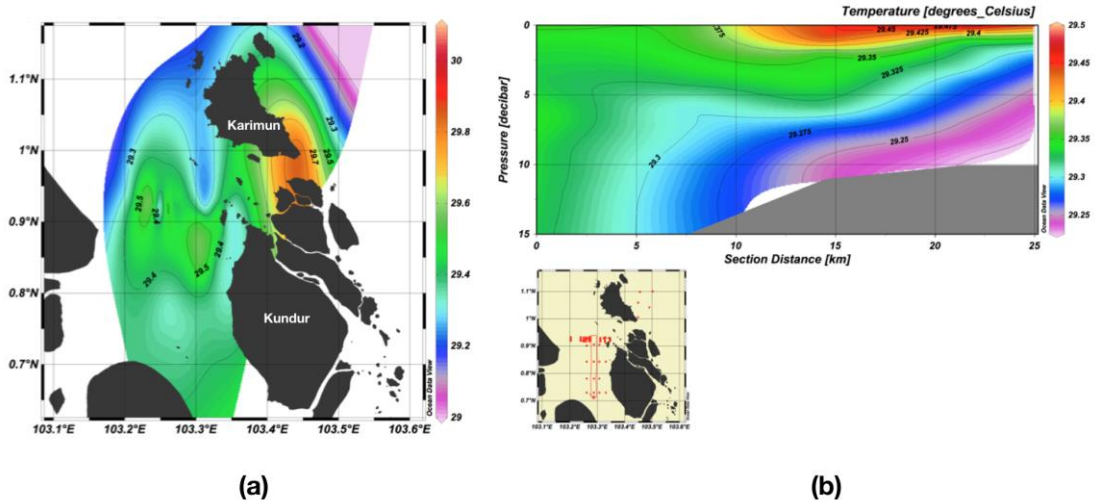


**Figure 7.** Sea surface temperature (a) and north-south section of sea surface temperature profile (b) ploted from survey data July 2012.

Salinity is the number of grams of salt in a kilogram of seawater indicating salt levels, which can now be measured by conductivity sensors that reflect electrical conductivity of seawater. Salinity parameter is as important as seawater temperature, as both parameters are able to explain physical phenomenons in the sea. Fig. 8a is a plot of salinity data from the measurement of CTD cast in the field. In contrast to the distribution of temperature, higher salinity (> 30.5 psu) was found on the northeast side where the seawater mass in the Singapore Strait is more dominated by the mass of water originating from the South China Sea, whereas at locations of mining activities, the surface salinity ranged from 25.5- 27.5 psu.

Cross-sectional of salinity distribution on the north - south transect (see insert in figure 8b) shows the same thing, i.e. there is no coating of water mass which is indicated by changes in salinity to depth. In the southern part and the northern part, there is water mass that has relatively higher salinity (> 27 psu), whereas in the middle part salinity value is lower (< 26 psu).

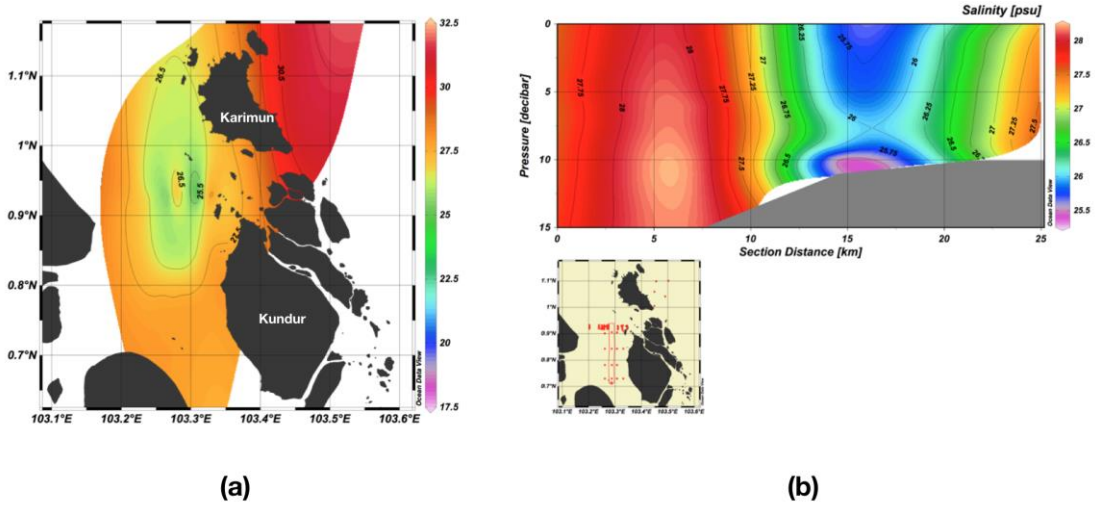


**Figure 8.** Sea surface temperature (a) and north-south section of sea surface temperature profile (b) ploted from survey data July 2012.

Regarding water turbidity there are several terminologies used, among them are water brightness or water clarity [8]. Brightness describes how deep sunlight can penetrate water and is affected by the process of absorption and scattering by sedimentary particles, detritus, algae, etc. [9].

As for units of turbidity, there are some examples like the JTU (Jackson Turbidity Unit). In 1970 Formazin a chemist discovered another example, which became a new standard of turbidity measurement so that the unit is called the FTU (Formazin Turbidity Unit), then there is also the NTU (Nephelometric Turbidity Unit), which is the most commonly used unit because in the calibration the tool uses two detectors [10,11].

As an illustration, an example is given of the conversion of turbidity to the total suspended solids (TSS). In Indonesia, the rules exist to see whether the waters have been polluted or not seen from the turbidity value. The parameter is TSS (Total Suspended Solid) expressed in mg/L units [10]. Figure 9 is an example of water with different turbidity expressed in both NTU and mg/L units. The conversion value is built from taking several water samples and measured with two different tools so as to produce a close correlation (confidence level> 95%). To get the TSS value (mg/L) from the turbidity value (NTU) then convert the regression equation y = 3.416x, where y is TSS and x is turbidity.

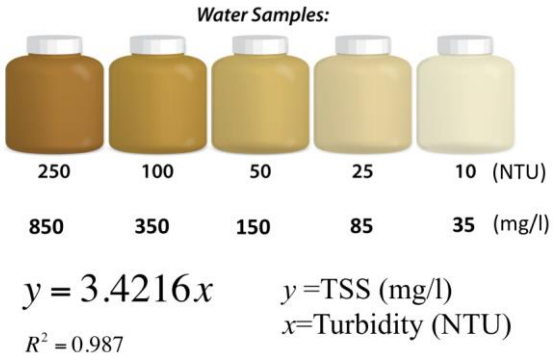


**Figure 9.** Convertion of NTU unit to become mg/L algorithm.

Figure 10a is the distribution of turbidity values plotted from measurement data at 7 points. Turbidity values ranged from 9.85- 10.75 NTU (which is the quality standard for marine biota according to Minister of Environment Decree No. 51 of 2004 is <5 NTU). When the turbidity value is converted to TSS value then the yield is 35-37 mg/L (TSS quality standard for seagrass and coral is 20 mg/L, while for mangrove 80 mg/L). The highest turbidity was seen in the west coast of Kundur Island, while the

area near Karimun and Bengkalis Island had lower turbidity. It can be seen that the turbidity waters in both the IUP Region and outside the IUP Region have exceeded the quality standard. Within IUP Timah, the contribution of turbidity might come from KK and KIP activities. While outside the IUP area the contribution of turbidity is thought to come from the rivers innate (including the Kampar River), and stirring of the seabed because mixing zone (mixed zoning) can reach the seabed.

Transverse distribution of depth can be seen in figure 10b. As an explanation of horizontal distribution, the mass of water with turbidity values is lower than that in the middle and south.

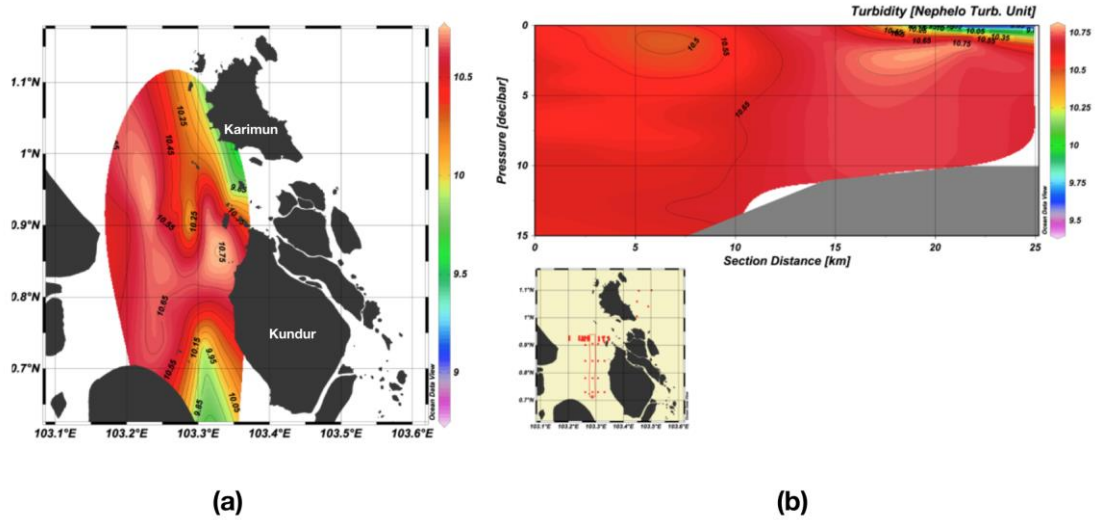


**Figure 10.** Sea surface turbidity (a) and north-south section of turbidity profile (b) ploted from survey data July 2012.

The northeast monsoon is frequently called as the west season that occurs in the Java Sea. On this season the dominant wind moves from the direction of the South China Sea, as can be seen in the inserted wind-rose image. At sea level ahead of the ebb and flow of water in the west coast waters of Kundur Island moving towards the Malacca Strait and the Singapore Strait to the Pacific Ocean. Current movement patterns are seen modified by the ranks of islands in the Riau Islands. Strong currents (indicated by longer vector lengths) appear to dominate the deep narrow straits. Current velocity can reach>20 cm/sec (figure 11).

When the sea level is at the lowest position (lowest ebb), the current pattern is still the same as before the low tide, as only the current velocity is seen to have decreased to> 60% so that the remaining <10 cm/sec (figure 11b).

Very different current pattern conditions are seen when the sea level is in the MSL (Mran Sea Level) position towards the highest tide point (figure 11c). In total the direction of movement of the current is reversed. Seawater mass was seen entering the western waters of Kundur Island from the north (Malacca Strait) and from the northeast (South China Sea through the Singapore Strait). The current velocity is around 30 cm/sec mainly in narrow straits (figure 11a).

When the sea level reaches the highest tide, in general the current still moves in the same pattern as when it goes to the tide, but the speed of the current appears to slow down (figure 11d). It is clear that the water mass near the coast (especially the east coast of Riau Province), flows into the coastal waters through the existing straits with a speed of < 20 cm/sec.

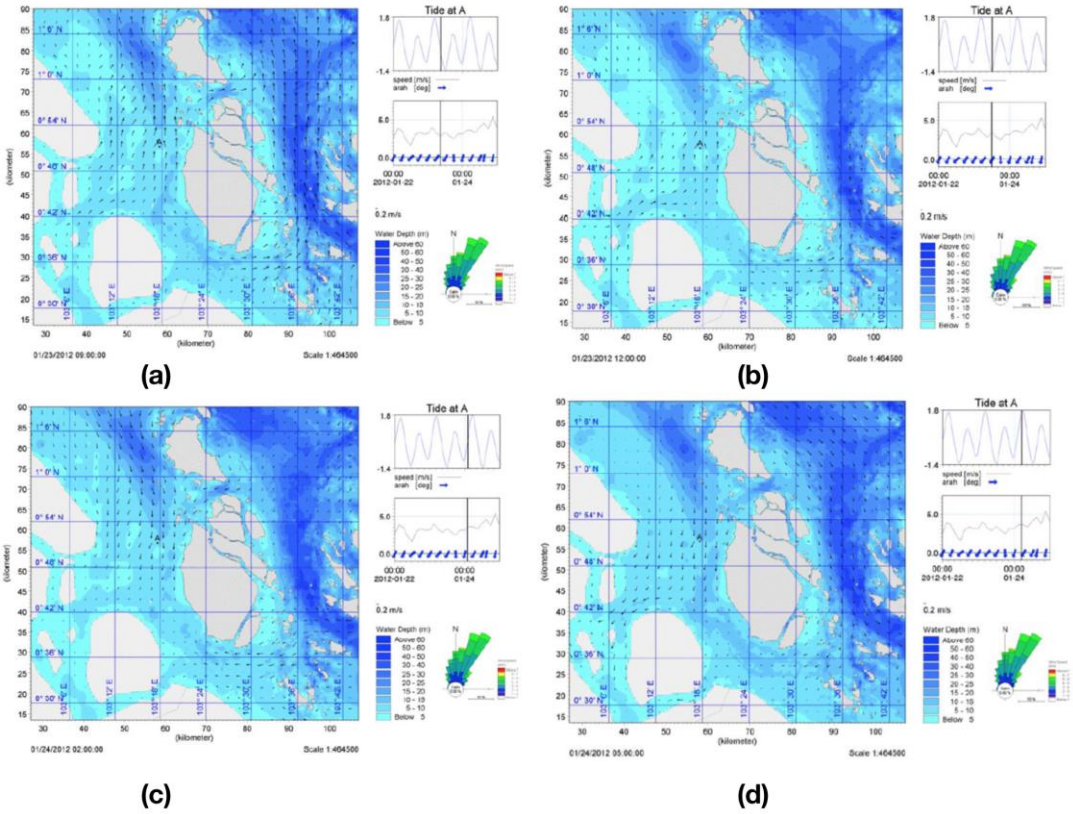


**Figure 11.** (a) The circulation pattern of current when the sea level is at msl towards the lowest receding point, (b) at the lowest ebb, (c) current circulation pattern when sea level is at MSL towards the highest tide point, and (d) highest tide point at the northeast monsoon.

The parameter that distinguishes between northeast and southeast monsoon is wind. In the southeast monsoon the inserted image (wind-rose) clearly shows that the dominant wind moves from the southeast.

Figure 12 is a current pattern image of 4 different sea level scenarios. Successively from figure 12a to figure 12d indicate that the current pattern at sea level at MSL goes to the lowest ebb, the lowest ebb point, current pattern at sea level at MSL to the highest tide and the sea level at the highest tide.

Western coast of Kundur waters are coastal waters and not open ocean, so the currents that occurred are more influenced by tides so that the current pattern in the 4 scenarios has a high similarity. When the tide moves from the Malacca Strait and the Singapore Strait, instead it goes out to the same strait.

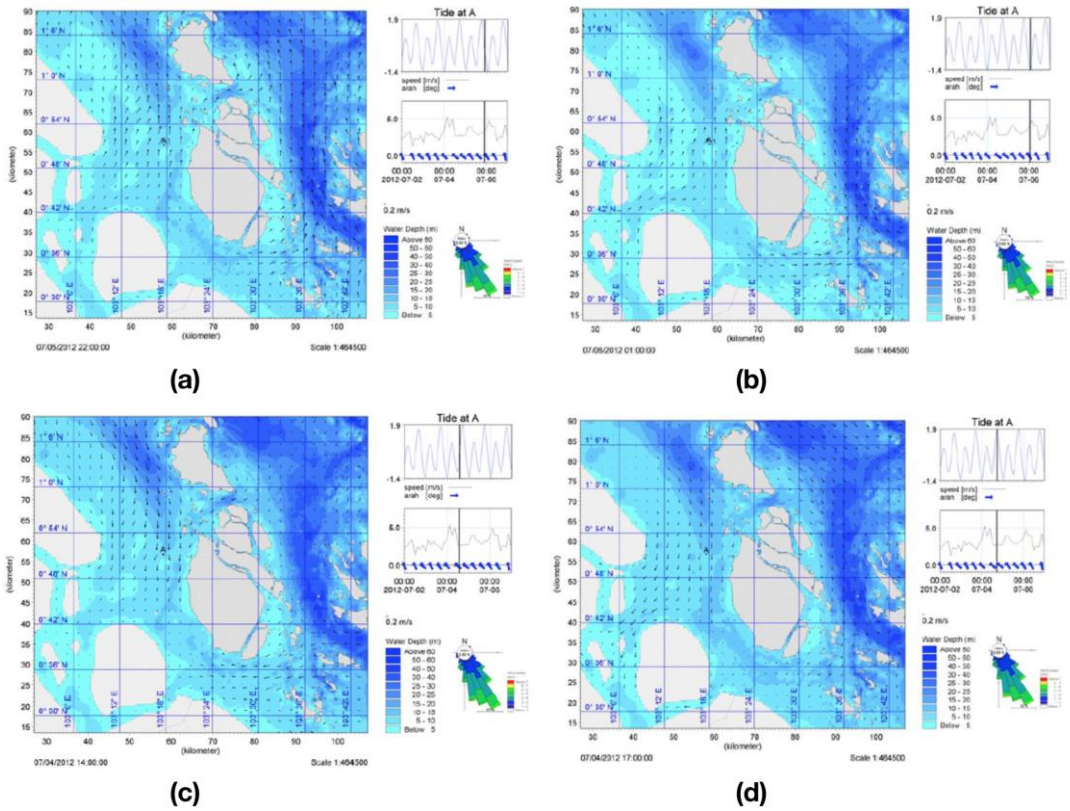


**Figure 12.** (a) The circulation pattern of current when the sea level is at MSL towards the lowest receding point, (b) at the lowest ebb, (c) Current circulation pattern when sea level is at MSL towards the highest tide point, and (d) highest tide point at the southeast monsoon.

Tin mining activities at sea by PT Tambang Timah by operating 6 dredgers and Suction vessels are able to generate and add turbidity values in the west coast of Kundur Island. The addition of turbidity caused by dredger and suction vessel activities is calculated and simulated by observing the hydrodynamic/current conditions and the sediment characteristics of the dredged seabed.

Besides that there are scenarios made in this 8 models, namely the sea level at low tide, the lowest ebb, near the high tide and the highest tide. Each of these conditions is also presented in two different seasons, namely the northeast and southeast seasons. Figure 13 and 15 are the simulation results of the eight scenarios plus two images in the maximum conditions in the northeast (figure 14) and southeast seasons (figure 16).

TSS distribution patterns resulting from sand mining activities in sea will follow the flow pattern that occurs at that location. As explained in the oceanographic section, the current pattern at low tide moves north and partly to the northeast towards the Malacca Strait and the South China Sea through the Singapore Strait. TSS distribution patterns also appear to have the same trend spreads to the north and northeast.

The addition of TSS due to the highest tin mining is seen at the point of location of the dredger and suction vessel which is marked with a dark yellow color which is around 0.09-0.1 kg/m or equivalent to 90 mg/L - 100 mg/L. So if you add the highest value of the TSS measurement, the TSS value of the waters around the dredger would be 137 mg/L.

When the sea level is at the lowest ebb position, the spread of TSS is wider but has not reached to the coastal of Karimun Besar Island (figure 13b). TSS distribution patterns at the time of the tide towards the highest tide point are presented in figure 13c. Because there is a strong tidal boost from the north, TSS spreads southward to the south of Kundur Island. When the tide push is already at a maximum,

when the highest tide, as if the mass of the water is held up and the TSS is more concentrated around the mining location, the TSS concentration will be higher (figure 13d).

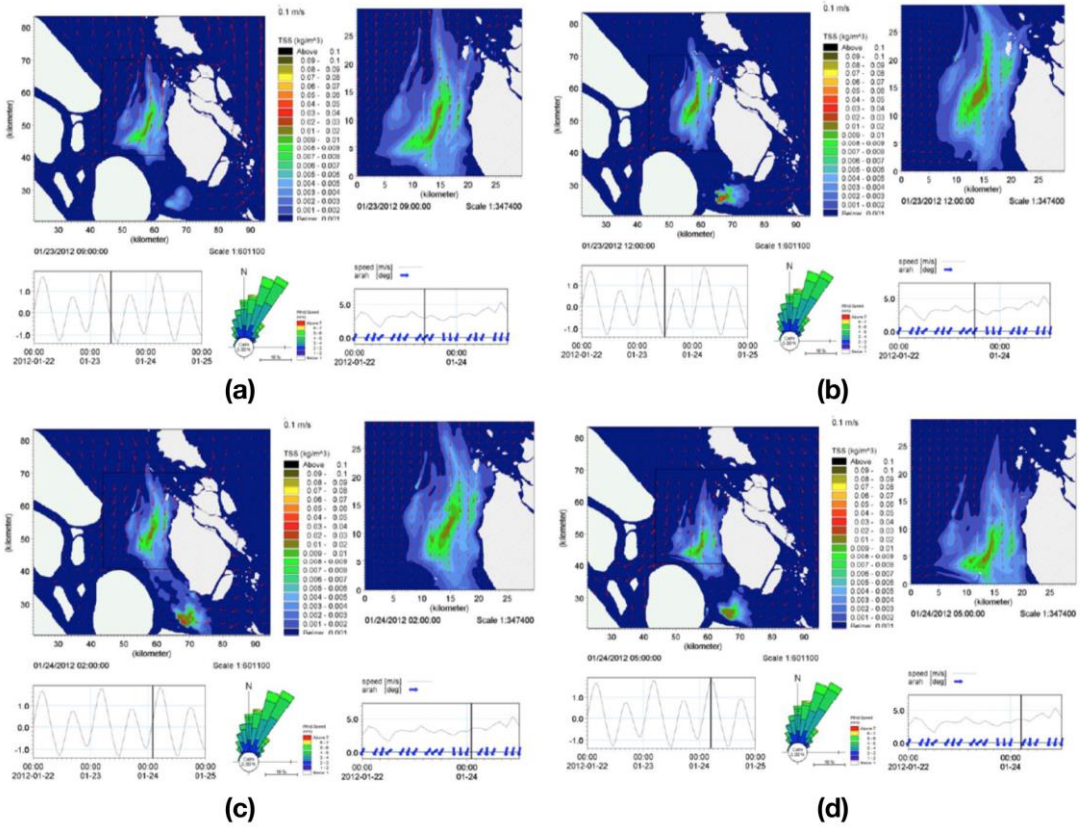


**Figure 13.** (a) TSS Distribution from mining activities when the sea level is at MSL towards the lowest receding point, (b) at the lowest ebb, (c) Current circulation pattern when sea level is at MSL towards the highest tide point, and (d) highest tide point at the northeast monsoon.

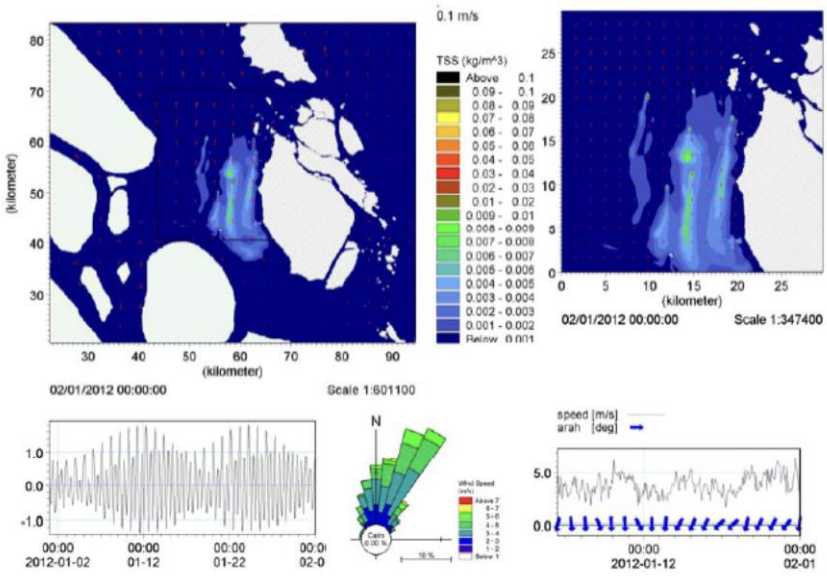


**Figure 14.** Exposed areas of maximum TSS distribution due to tin mining activities in the west coast waters of Kundur Island, in the northeast season, for one month running model.

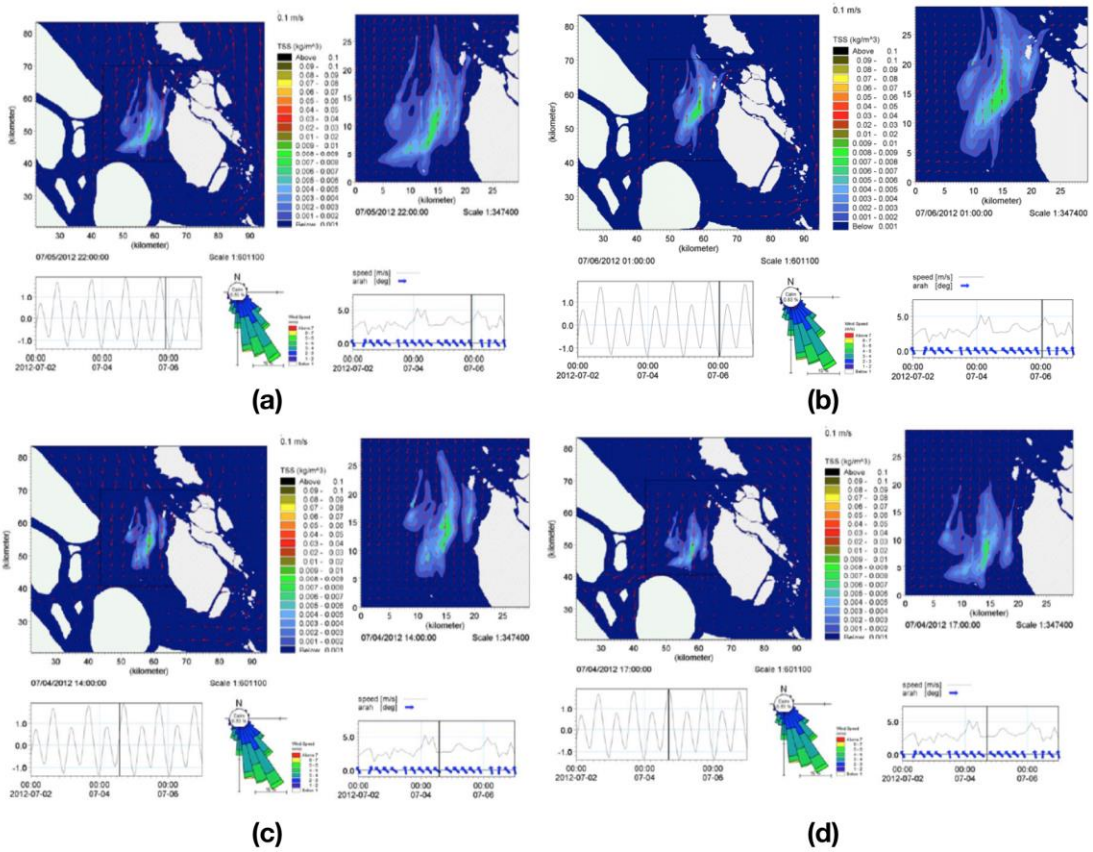


**Figure 15.** (a) TSS Distribution from mining activities when the sea level is at MSL towards the lowest receding point, (b) at the lowest ebb, (c) Current circulation pattern when sea level is at MSL towards the highest tide point, and (d) highest tide point at the southeast monsoon.

As we know that one of the characteristics of sediment compared to water is that the density of sediment is heavier than the density of water, after one month of simulation there was an addition of sediment on the seabed because TSS slowly settles so that the concentration of TSS in the water column slowly decreases (figure 14). The IUP (Mining Business Permit) of PT Tambang Timah which operates west of Kundur Island and southwest of Karimun Island produces limited TSS distribution on the west side because the influence of the northeast wind is not optimal.

Winds in the southeast monsoon contribute significantly to the TSS distribution area caused by tin mining activities in the west coast waters of Kundur Island, as shown on figure 15.

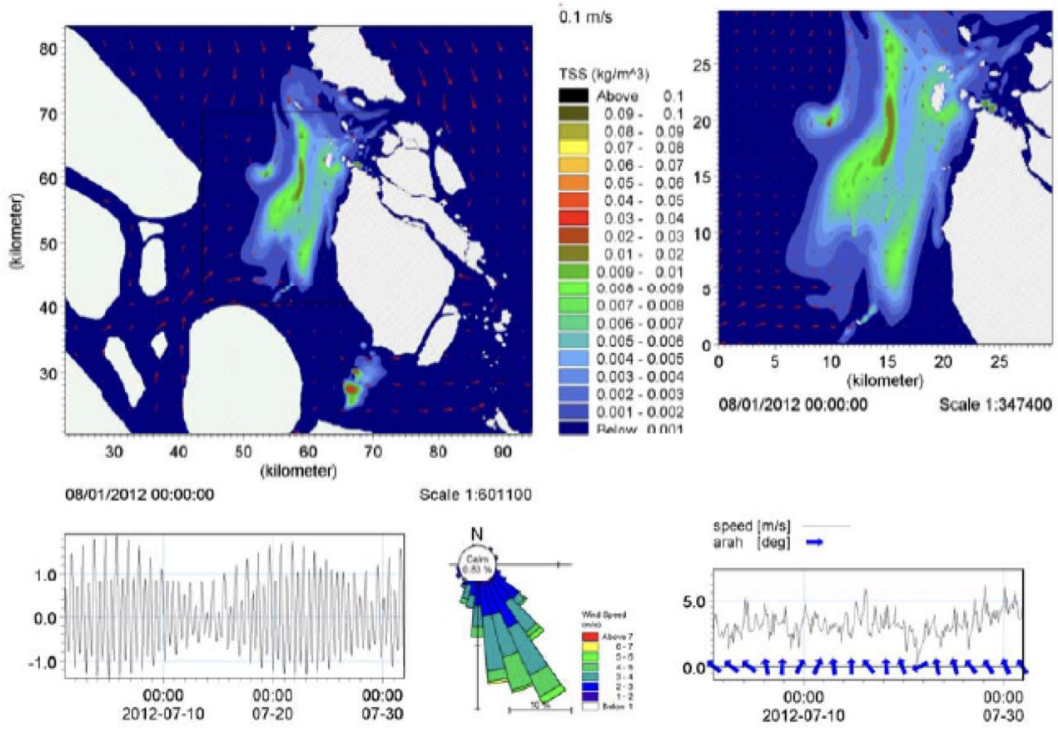


**Figure 16.** Exposed areas of maximum TSS distribution due to tin mining activities in the west coast waters of Kundur Island, in the southeast season, for one month running model.

The distribution of TSS due to mining activities during the southeast season is more extensive than the distribution of TSS during the northeast season (figure 16). Besides that the distribution of higher TSS concentration values of >20 mg/L (concentrated green color) during the southeast season looks wider than the northeast season. However, the distribution of TSS does not reach the coast, as its distribution tends to be in the north, a small portion enters the small strait between Karimun Island and Kundur Island.

## 4. Conclusion

Without lead mining at sea, the turbidity value of Kundur Island has reached a value of 9.85-10.75 NTU (TSS value is 35-37 mg/L). The highest turbidity was seen on the west coast of Kundur Island, while the waters near Karimun Island and Bengkalis had lower turbidity. Turbidity levels (or TSS) of the waters west of Kundur Island are also influenced by (a) the presence of river flows from the mainland of Sumatera, especially the Kampar River, which empties into the Berhala Strait and is directly related to the western waters of Kundur Island; and (b) the existence of natural phenomenons, namely the mixing zone that reaches the bottom of the ocean waters (the depth ranges from 5-24 m), as a result of the convergence of river flows from the Sumatran mainland, and the Kundur coastal waters. Regarding the quality standards used, there are different interpretations of the magnitude of the impact of KK operations and KIP. In addition, mining operations by 6 KK and KIP have added turbidity to the waters - which when converted to TSS - amounted to 0.09-0.1 kg/m (highest value), or equivalent to 90-100 mg/L. Hence, it can be said that tin mining operations have added to the TSS value of the west coast waters of Kundur Island which is now 125-137 mg/L. Regarding the quality standards used, this situation brings different interpretations of the magnitude of the impact of KK operations and KIP.

**Acknowledgements**

We would like to say thank PT. Timah, Kundur Indonesia have been facilitated us during field survey. Appresiation are also address to Mr. Djatmiko from Oceanography Research Center, Jakarta to help us on data collecting.

**References**

[1] Newell R C, Seiderer L L and Hitchcock D.R. 1998 The impact of dredging works in coastal waters: A review of the sensitivity to disturbance and subsequent recovery of biological resources on the sea bed *Oce. Mar. Biol. Annual Rev.* **36** 127-178
[2] Lund-Hansen L C, Petersson M and Nurjaya W 1999 Vertical sediment fluxes and wave-induced resuspension in a shallow-water coastal lagoon *Estuaries* **22** 39-46
[3] Wyrtki 1961 Physical Oceanography of the Southeast Asian Waters (La Jolla: The University of California)
[4] Extension U W 2003 Turbidity: A water clarity measure Water Action Volunteers: Volunteer Monitoring Factsheet Series University of Wisconsin
[5] Bishop J K B 1986 The correction and suspended particulate matter calibration of Sea Tech transmissometer data *Deep-Sea Res.* **33** 121-134
[6] Boss E, Taylor L, Sherry, Gilbert, Gundersen K, Hawley N, Janzen C, Johengen T, Purcell H, Robertson C, Schar D W, Smith G J and Tamburril M N 2009 Comparison of inherent optical properties as a surrogate for particulate matter concentration in coastal waters *Limnol. Oceanogr. Methods* **7** 803-810
[7] Guillén J, Palanques, Puig, Durrieu de madron and Nyffeler F 2000 Field calibration of optical sensors for measuring suspended sediment concentration in the western Mediterranean *SCI. MAR.* **64** 427-435
[8] Zaneveld J R V, Richard W S and Bartz R 1979 Optical properties of turbidity standards *SPIT* **208** *Ocean Optics* V/1-159
[9] Kitchen J C, Zaneveld J R V and Pak H 1982 Effect of particle size distribution and chlorophyll content on beam attenuation spectra *Applied Optics* **21** 3913-3918
[10] Nurjaya I W 1996 Sediment resuspension due to tue wave and tide in Ronbjerg, Denmark [Thesis] (Denmark: Marine Science Program Arhus University)
[11] Yentsch C S, Cullen J J, Lapointe B, Phinney D A and Yentsch S W 2002 Sunlight and water transparency: cornerstones in coral research *J. Exp. Mar. Biol. Ecol.* **268** 171–183
[12] Weber-Scannell O K and Duffy L K 2007 Effects of total dissolved solids on aquatic organisms: a review of literature and recommendation for salmonid species. *American J. Env. Sci.* **3** 1- 6
[13] Leonard B P 1991 The ultimate conservative difference scheme applied to unsteady one-dimensional advection (North Holland: Elsevier Science Publishers B.V)
[14] Krone R B 1962 Flume studies of the transport of sediment in estuarial shoaling processes *Tech.l Rep., Hydr. Eng. Lab.* (Barkeley: University of California)
[15] Rijn L C 1984 Sediment transport, part II suspended load transport *J. Hydr. Eng.* **110**
[16] Yalin M S 1972 Mechanics of sediment transport (Hendington Hill Hall: Pergamon Press Ltd)
[17] Engelund F and Fredsoe J 1976 A sediment transport model for straight alluvial channels *Nordic Hydrology* **7** 293 – 306